



## Article

# Comparing Composition Control Structures for Kaibel Distillation Columns

Yang Yuan , Kejin Huang \*, Haisheng Chen, Xing Qian , Lijing Zang, Liang Zhang and Shaofeng Wang

College of Information Science and Technology, Beijing University of Chemical Technology, Beijing 100029, China; yuanyang@mail.buct.edu.cn (Y.Y.); chenhs@mail.buct.edu.cn (H.C.); qianx@mail.buct.edu.cn (X.Q.); 2019400169@mail.buct.edu.cn (L.Z.); zhangl@mail.buct.edu.cn (L.Z.); sfwang@mail.buct.edu.cn (S.W.)

\* Correspondence: huangkj@mail.buct.edu.cn; Tel.: +86-10-64437805; Fax: +86-10-64437805

Received: 2 December 2019; Accepted: 10 February 2020; Published: 13 February 2020



**Abstract:** Although Kaibel distillation columns are superior to conventional distillation sequences owing to smaller equipment investment and operation cost, they display high nonlinearity and this greatly increases the difficulty of achieving their tight control. To overcome this problem, four decentralized composition control structures, i.e., the  $CS_{R/QR}$ ,  $CS_{R/B}$ ,  $CS_{D/QR}$ , and  $CS_{D/B}$  structures, are proposed and compared based on the control of a Kaibel distillation column fractionating a methanol/ethanol/propanol/butanol quaternary mixture. These four composition control structures all include five composition control loops. While the four of them are employed to maintain the purity of the top, upper sidestream, lower sidestream, and bottom products, the remaining one is employed to minimize the energy consumption of the Kaibel distillation column by maintaining the composition of propanol at the first stage of the prefractionator. Dynamic simulation results show the  $CS_{R/QR}$  and  $CS_{R/B}$  structures can tightly maintain the purity of the controlled products with a small overshoot and short settling time after facing various disturbances in feed conditions, but the  $CS_{D/QR}$  and  $CS_{D/B}$  structures lead to oscillatory responses (the latter even shows divergent responses under individual disturbances). At the end of the article, some effective guides for developing composition control systems are given.

**Keywords:** Kaibel distillation column; PID; DWDC; process control; composition control

## 1. Introduction

In order to lessen the energy consumption of distillation processes effectively, various process intensification technologies have been proposed and dividing-wall distillation columns (DWDCs, c.f., Figure 1a) are the most famous of them all [1–6]. As a special sort of DWDCs separating quaternary mixtures, Kaibel distillation columns (c.f., Figure 1b) can reduce equipment investment and operation cost by about 40%, respectively, with reference to conventional direct, indirect and discrete distillation sequences. Moreover, the Kaibel distillation column has the simplest topological structure in all four-component DWDCs, so it is most likely to be applied in industry and deserves to be deeply studied [7–10].

There are three noteworthy differences between the Kaibel distillation column and the conventional three-component DWDC: (1). The former separates quaternary mixtures but the latter separates ternary mixtures; (2). The former includes two sidestream products that are significantly coupled each other but the latter includes only one sidestream product; (3). Remixing effect is completely eliminated in the latter but still slightly existed in the former [11]. From the three differences above, it is not difficult to deduce a fact that the nonlinear degree of the Kaibel distillation column is higher than that of the conventional three-component DWDC. This fact implies that tightly controlling the purity of

products is more difficult for the Kaibel distillation column than for the conventional three-component DWDC [12–16] and also explains why studies on the dynamic control of the Kaibel distillation column are so few thus far. For the control of a small experimental Kaibel distillation column built to separate a methanol(M)/ethanol(E)/propanol(P)/butanol(B) (MEPB) quaternary mixture, Dwivedi et al. proposed a temperature control structure including the top, upper sidestream, lower sidestream, and prefractionator temperature control loops [17]. According to the experimental simulation results obtained, the temperature control structure could guarantee the stable run of the Kaibel distillation column after facing various disturbances. Qian et al. compared three decentralized control structures, i.e., a temperature control structure, a composition-temperature cascade control structure, and a composition control structure, based on the control of a Kaibel distillation column separating a MEPB quaternary mixture (MEPB Kaibel distillation column) [18]. In terms of their results, the temperature control structure was superior to the composition-temperature cascade control structure and the composition control structure because of better dynamic characteristics and rather small steady-state deviations in the controlled products. Fan et al. compared three temperature control structures in terms of the operation of a Kaibel distillation column fractionating an n-pentane/n-hexane/n-heptane/n-octane quaternary mixture [19]. While the first temperature control structure includes only the top, upper sidestream, and lower sidestream temperature control loops, the second and third control structures add, respectively, an additional top prefractionator temperature control loop and a bottom prefractionator temperature control loop on the foundation of the first temperature control structure. Closed-loop evaluation results showed that the first temperature control structure could not guarantee the stable run of the Kaibel distillation column after facing various disturbances but the other two control structures could, which demonstrated the necessity of adding a prefractionator temperature control loop. To fractionate a benzene/toluene/xylene/heavies quaternary mixture, Tututi-Avila et al. developed a Kaibel distillation column using a genetic algorithm and demonstrated its capability in energy saving [8]. Furthermore, they gave a composition control structure including five composition control loops to control the developed Kaibel distillation column. Recently, Pan et al. proposed a temperature control structure with pressure compensated for the operation of the Kaibel distillation column [20], and Qian et al. proposed a composition-temperature cascade control structure through combining model predictive control and conventional PI control [21]. It is not difficult to see from the above analyses that the researches on the dynamic control of the Kaibel distillation column are not only small in amount but also limited to temperature inferential control to a certain degree. Although it is hard to deny that temperature inferential control is easier to achieve than composition control from an engineering perspective, temperature inferential control cannot completely eliminate the steady-state deviations in the controlled products.

In the current article, we will deeply study the composition control of the Kaibel distillation column. Firstly, four composition control structures using PI controller are proposed. Then, the comparison between these four composition control structures is carried out based on the operation of a MEPB Kaibel distillation column. Finally, some effective guidelines for developing the Kaibel distillation column composition control system are derived.

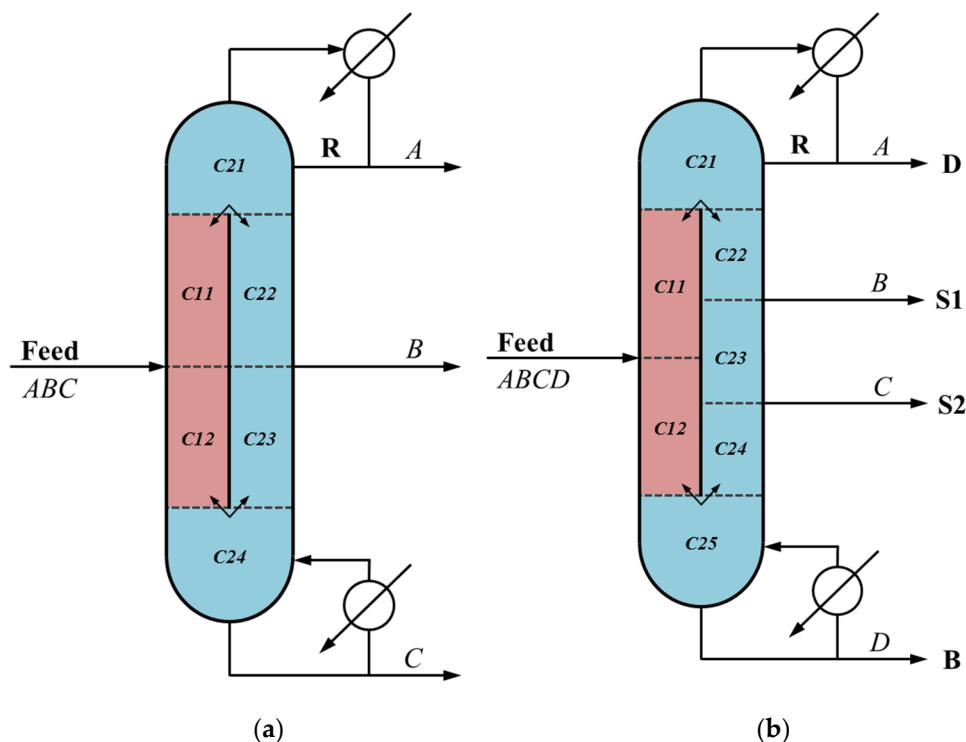


**Figure 1.** Two sorts of dividing-wall distillation columns (DWDCs): (a) Conventional three-component DWDC; (b) Kaibel distillation column.

## 2. Four Composition Control Structures Proposed for the Control of the Kaibel Distillation Column

For the Kaibel distillation column, there are a total of eight operation degrees of freedom, including distillation flow rate  $D$ , reflux flow rate  $R$ , upper sidestream flow rate  $S1$ , lower sidestream flow rate  $S2$ , reboiler heat duty  $Q_R$ , bottom product flow rate  $B$ , liquid split ratio  $R_L$ , and vapor split ratio  $R_V$ . Due to the fact that the position of the dividing wall is usually fixed,  $R_V$  is generally kept constant during the dynamic process and there are actually seven manipulated variables left. In line with the theory proposed by Skogestad that a complete control system should be divided into three levels [22], the seven manipulated variables of the Kaibel distillation column are divided into three groups (c.f., Figure 2). The first group contains two manipulated variables ( $D/R$  and  $Q_R/B$ ), which are employed to control the liquid levels of the reflux tank as well as the bottom sump and therefore to stabilize the Kaibel distillation column. The second group contains four manipulated variables ( $D/R$ ,  $S1$ ,  $S2$ , and  $Q_R/B$ ), which are used to maintain the purity of the top, upper sidestream, lower sidestream, and bottom products. The third group contains one manipulated variable ( $R_L$ ), which is used to achieve the self-optimizing control of the Kaibel distillation column. Through appropriately combining the three groups of manipulated variables, four composition control structures, i.e., the  $CS_{R/Q_R}$ ,  $CS_{R/B}$ ,  $CS_{D/Q_R}$ , and  $CS_{D/B}$  structures, can be obtained and shown in Figure 3a–d, respectively. They are named by the term of “ $CS_{X/Y}$ ” (The subscripts of  $X$  and  $Y$  denote, respectively, the manipulated variables of the top and bottom control loops). For these four composition control structures, proximity principle is employed to pair manipulated variables and controlled variables to shorten the response time of each control loop. Namely, the top, upper sidestream, lower sidestream, bottom, and prefractionator control loops employ, respectively,  $D/R$ ,  $S1$ ,  $S2$ ,  $Q_R/B$  and  $R_L$  as manipulated variable and the composition of impure component  $E$  in the top product, component  $E$  in the upper sidestream product, component  $P$  in the lower sidestream product, impure component  $P$  in the bottom product, and component  $P$  at the first stage of the prefractionator as controlled variable. In particular, tightly maintaining the composition of component  $P$  at the first stage of the prefractionator can prevent the component  $P$  spilling over the top of the prefractionator enters the main column and therefore helps the Kaibel

distillation column working near the optimum operating point, which has been demonstrated by Ling and Luyben [23].

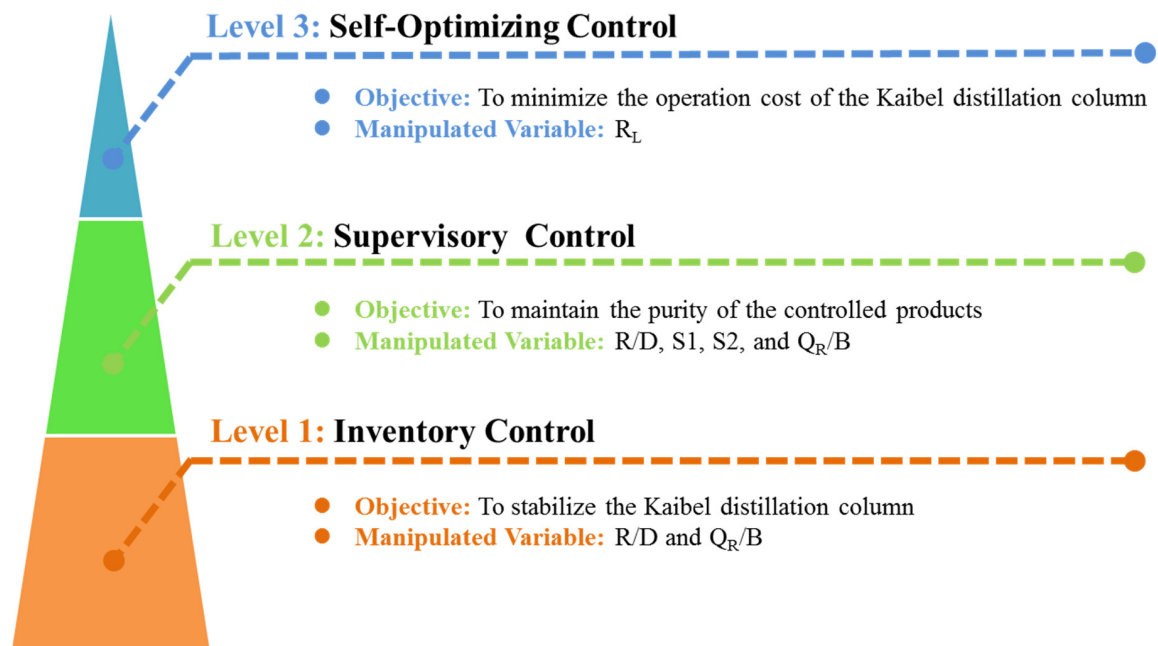


Figure 2. Three levels of the composition control system for the control of the Kaibel distillation column.

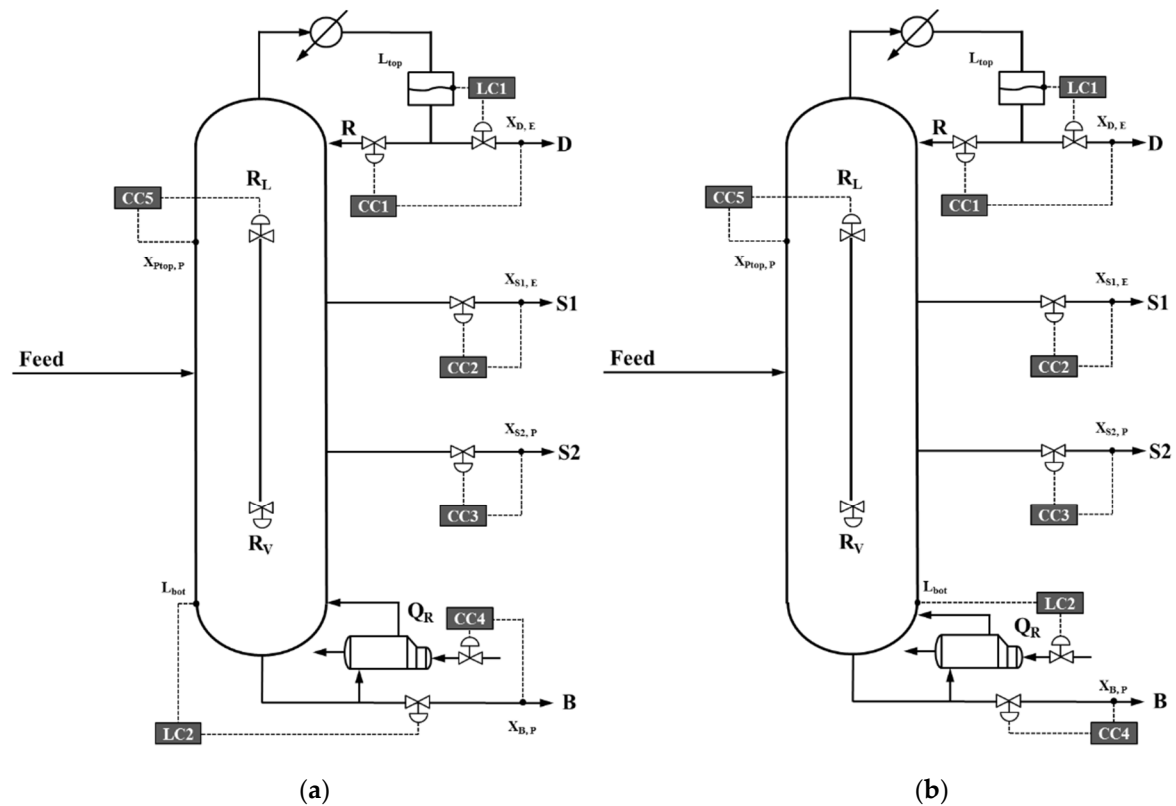
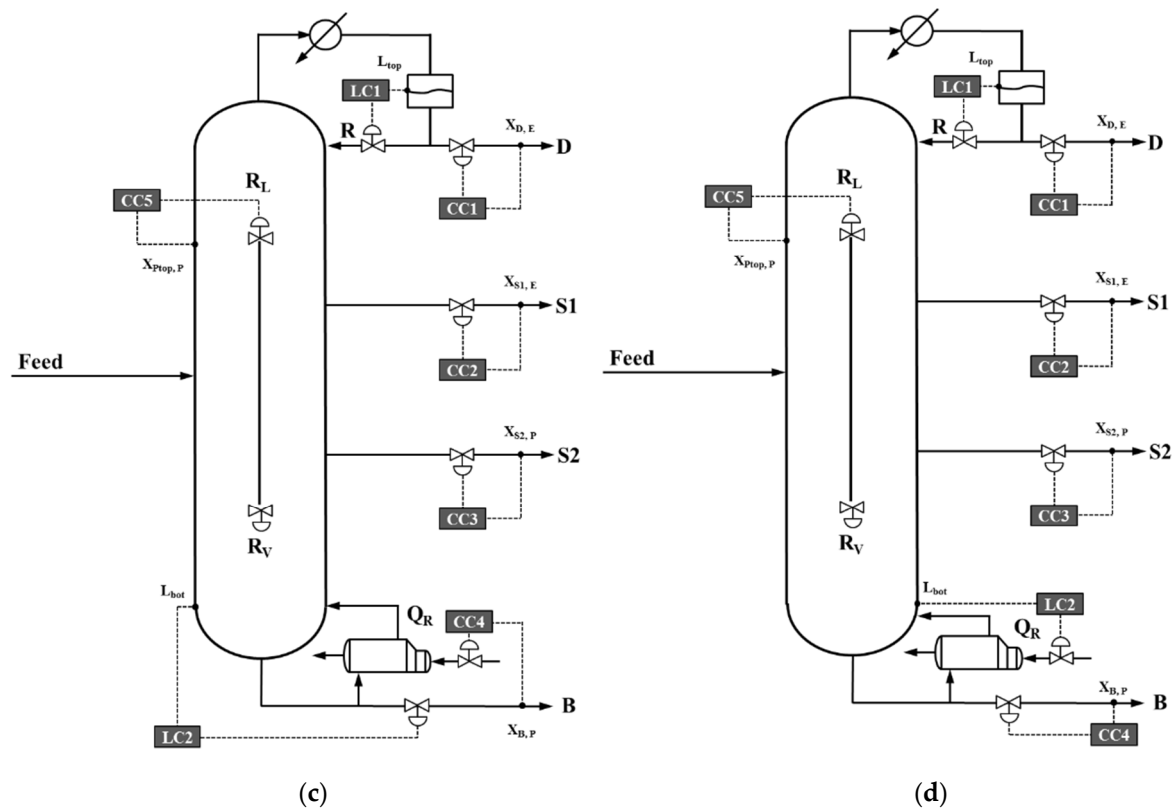


Figure 3. Cont.



**Figure 3.** Composition control structures proposed for the control of the Kaibel distillation column: (a)  $CS_{R/QR}$  structure; (b)  $CS_{R/B}$  structure; (c)  $CS_{D/QR}$  structure; (d)  $CS_{D/B}$  structure.

### 3. Comparing the $CS_{R/QR}$ , $CS_{R/B}$ , $CS_{D/QR}$ , and $CS_{D/B}$ Structures in Terms of the Control of a MEPB Kaibel Distillation Column

#### 3.1. Derivation of a MEPB Kaibel Distillation Column

Because the MEPB quaternary mixture is one of the most frequently studied quaternary mixtures in research field on the operation and control of the Kaibel distillation column, it is also selected in the current article for the convenience of comparing with previous research conclusions. The nominal volatility ranking of the four components M, E, P, and B is  $\alpha_M > \alpha_E > \alpha_P > \alpha_B$ . The design specifications to the MEPB Kaibel distillation column are given in Table 1. Aspen Plus and Aspen Dynamic are, respectively, employed to conduct the steady-state and dynamic simulations. Since there is no available Kaibel distillation column module in Aspen Plus, we have to use a combination of four Redfrac modules to simulate it (c.f., Figure 4). The NRTL property model is employed to simulate the characteristics of the MEPB quaternary mixture and thus to ensure the accuracy of simulation results as much as possible. A simple sequential search algorithm (As shown in Figure S1 of Supporting Information, it is extremely similar to the one proposed in our previous work for the synthesis and design of the conventional three-component DWDC [24]) is used to derive the optimum MEPB Kaibel distillation column. The total annual cost (TAC) representing the sum of operation cost and annual capital investment is selected as the economical objective function. In Figure 5a, the optimum MEPB Kaibel distillation column is shown. The main column and prefractionator of the MEPB Kaibel distillation column contain 70 and 40 stages, respectively. The equimolar saturated liquid feed is fed on stage P40 (The prefix P denotes the prefractionator) and the top, upper sidestream, lower sidestream, and bottom products are withdrawn from stages 1, 30, 50, and 70, respectively. Figure 5b shows the liquid composition profiles of the prefractionator and main column of the MEPB Kaibel distillation column. It can be seen that the quaternary mixture (M/E/P/B) is firstly separated into two ternary mixtures (M/E/P and E/P/B) in the prefractionator, and then separated into four pure products in the main column. Table S1 lists



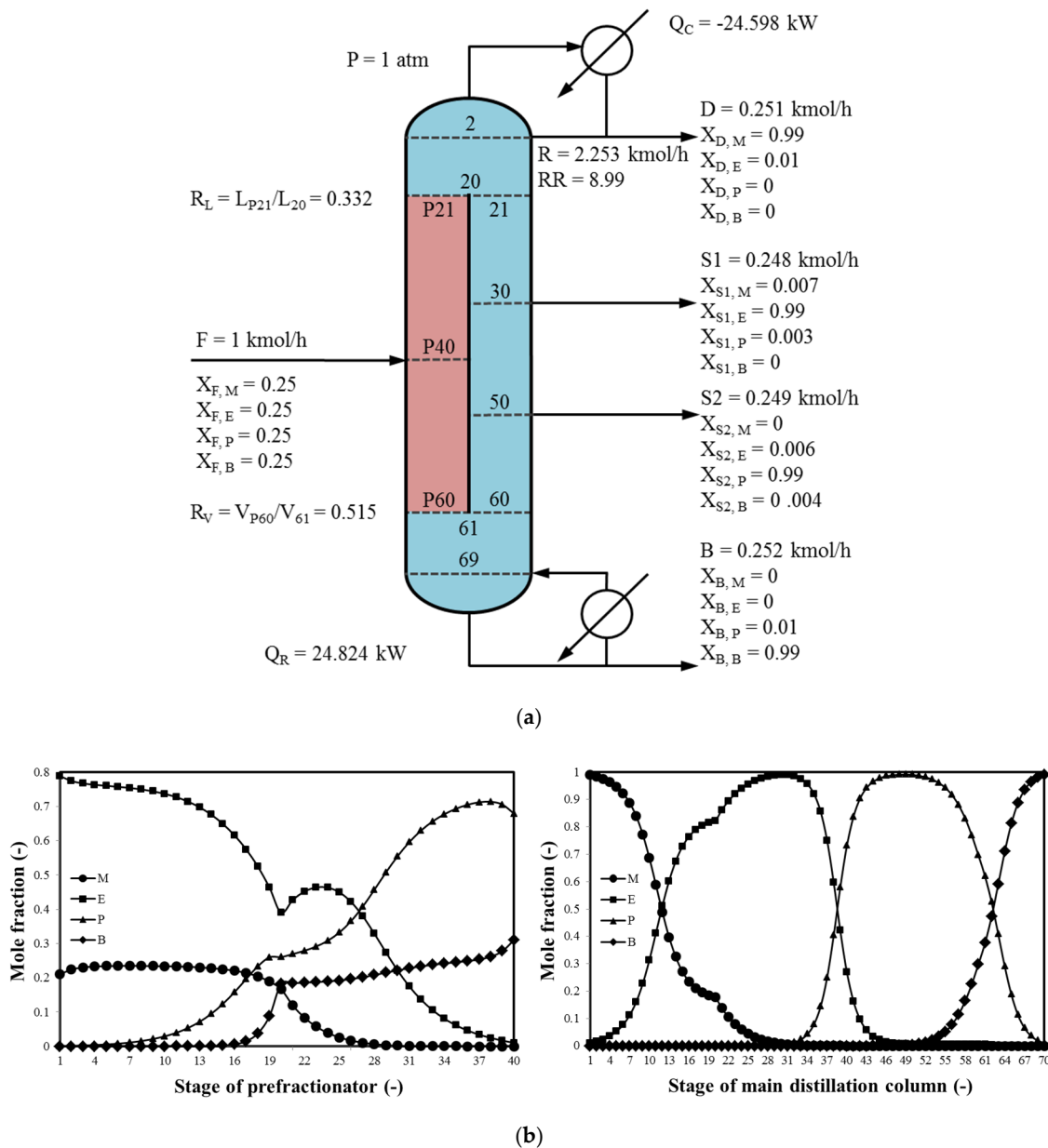


**Figure 5.** The optimum MEPB Kaibel distillation column and its static composition profiles: (a) MEPB Kaibel distillation column; (b) liquid composition profiles.

### 3.2. Tuning of Controller Parameters

For the  $CS_{R/Q_R}$ ,  $CS_{R/B}$ ,  $CS_{D/Q_R}$ , and  $CS_{D/B}$  structures, the two liquid level control loops use pure proportional controllers as well as the five composition control loops use proportional-integral (PI) controllers. Each composition measurement is assumed to involve a 3-min time delay. The tuning of composition controller parameters is carried out by the Tyreus-Luyben tuning rule built in Aspen Dynamic, and at least three rounds are done to ensure the fairness of the obtained comparison results. More specifically, the tuning of composition controller parameters can be divided into three steps: firstly, set all composition controllers to manual mode; secondly, tune the composition controllers one by one in an order as the top, bottom, upper sidestream, lower sidestream, and prefractionator control loops, and set the controllers to auto mode once their tuning have been completed; finally, as the order mentioned in the last step, tune cyclically the controller parameters until the controller parameters obtained in the current round are close to the controller parameters obtained in the previous round. In Table 2, the controller parameters of the  $CS_{R/Q_R}$ ,  $CS_{R/B}$ ,  $CS_{D/Q_R}$ , and  $CS_{D/B}$  structures are tabulated.



**Table 2.** Controller Parameters of the  $CS_{R/QR}$ ,  $CS_{R/B}$ ,  $CS_{D/QR}$ , and  $CS_{D/B}$  Structures.

Scheme	Controller	Manipulated Variable	Controlled Variable	$K_C$ (–)	$T_I$ (min)
$CS_{R/QR}$	CC1	R	$X_{D,E}$	0.08	113.52
	CC2	S1	$X_{S1,E}$	46.36	79.2
	CC3	S2	$X_{S2,P}$	113.74	39.6
	CC4	$Q_R$	$X_{B,P}$	0.05	54.12
	CC5	$R_L$	$X_{Ptop,P}$	0.19	46.2
	LC1	D	$L_{top}$	2	9999
	LC2	B	$L_{bot}$	2	9999
$CS_{R/B}$	CC1	R	$X_{D,E}$	0.69	145.2
	CC2	S1	$X_{S1,E}$	60.3	66
	CC3	S2	$X_{S2,P}$	116.73	39.6
	CC4	B	$X_{B,P}$	0.05	51.48
	CC5	$R_L$	$X_{Ptop,P}$	0.15	64.68
	LC1	D	$L_{top}$	2	9999
	LC2	$Q_R$	$L_{bot}$	2	9999
$CS_{D/QR}$	CC1	D	$X_{D,E}$	0.09	96.36
	CC2	S1	$X_{S1,E}$	46.78	79.2
	CC3	S2	$X_{S2,P}$	122.63	39.6
	CC4	$Q_R$	$X_{B,P}$	0.48	92.4
	CC5	$R_L$	$X_{Ptop,P}$	0.16	59.4
	LC1	R	$L_{top}$	2	9999
	LC2	B	$L_{bot}$	2	9999
$CS_{D/B}$	CC1	D	$X_{D,E}$	0.76	145.2
	CC2	S1	$X_{S1,E}$	62.36	72.6
	CC3	S2	$X_{S2,P}$	125.2	39.6
	CC4	B	$X_{B,P}$	0.64	79.2
	CC5	$R_L$	$X_{Ptop,P}$	0.15	64.68
	LC1	R	$L_{top}$	2	9999
	LC2	$Q_R$	$L_{bot}$	2	9999

### 3.3. Closed-Loop Evaluations of the $CS_{R/QR}$ , $CS_{R/B}$ , $CS_{D/QR}$ , and $CS_{D/B}$ Structures

Figure 6 displays the dynamic responses of the top control loop of the MEPB Kaibel distillation column controlled, respectively, under the  $CS_{R/QR}$ ,  $CS_{R/B}$ ,  $CS_{D/QR}$ , and  $CS_{D/B}$  structures in the face of a  $\pm 5\%$  variation in M feed composition. While the black curves corresponding to the positive disturbances, the grey curves corresponding to the negative disturbances. For the  $CS_{R/QR}$  and  $CS_{R/B}$  structures, the MEPB Kaibel distillation column works well and the composition of the controlled components of the top, upper sidestream, lower sidestream, bottom, and prefractionator products can smoothly return back to their nominal steady state values after a settling time of about 8 to 10 h. Additionally, the manipulated variables can quickly reach new stable values. For the  $CS_{D/QR}$  and  $CS_{D/B}$  structures, although the composition of the controlled components can also return back to their nominal steady state values, the settling times are extremely long, longer than 20 h, and oscillatory responses occur. Moreover, the oscillation degree of the  $CS_{D/B}$  structure is more serious than that of the  $CS_{D/QR}$  structure.



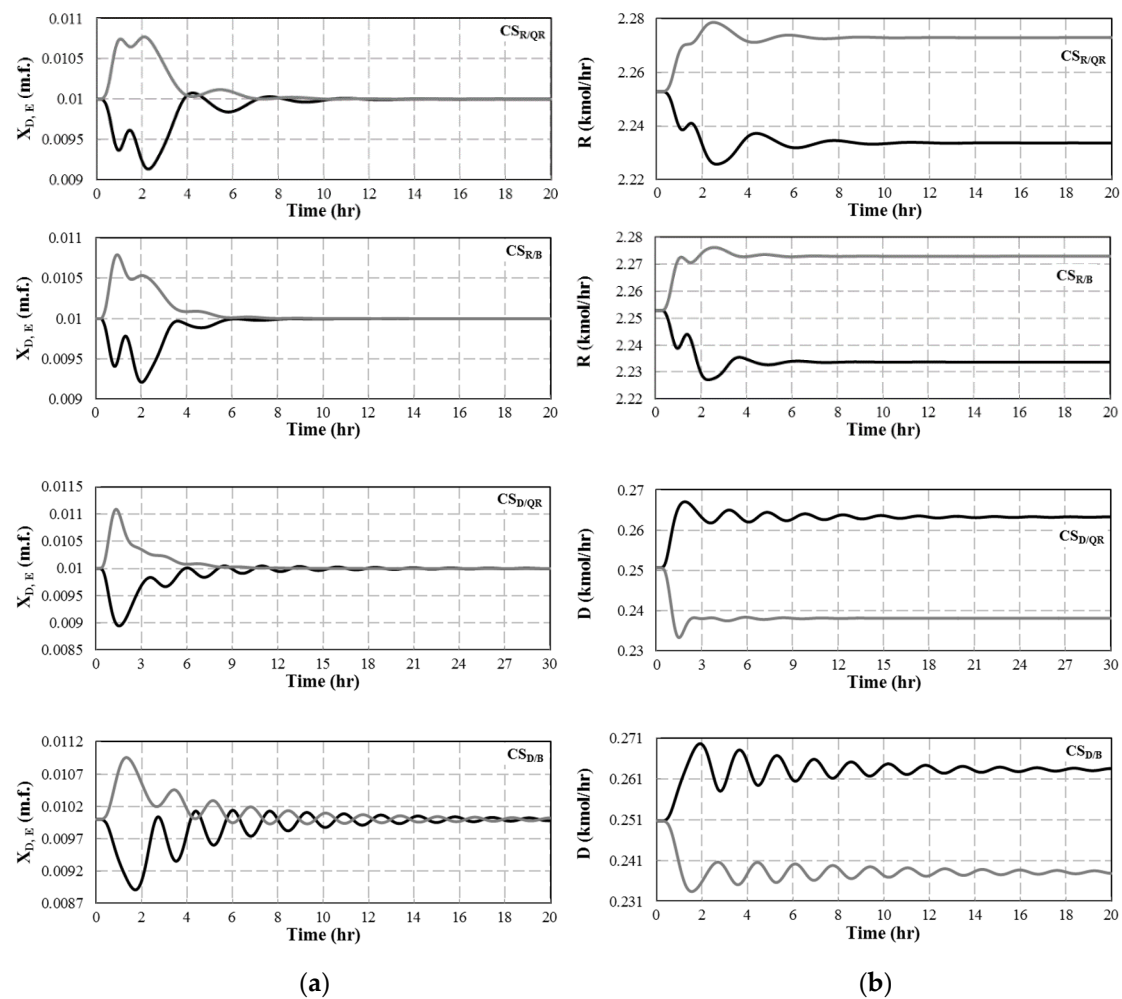


**Figure 6.** Dynamic responses of the top control loop of the MEPB Kaibel distillation column controlled, respectively, under the  $CS_{R/QR}$ ,  $CS_{R/B}$ ,  $CS_{D/QR}$ , and  $CS_{D/B}$  structures after facing a  $\pm 5\%$  variation in M feed composition (+5%: black curves and -5%: grey curves): (a) controlled variables; (b) manipulated variables.

Figure 7 gives the dynamic responses of the top control loop of the MEPB Kaibel distillation column controlled, respectively, under the  $CS_{R/QR}$ ,  $CS_{R/B}$ ,  $CS_{D/QR}$ , and  $CS_{D/B}$  structures in the face of a  $\pm 5\%$  variation in E feed composition. The  $CS_{R/QR}$  and  $CS_{R/B}$  structures still do a nice job to guarantee the stable run of the MEPB Kaibel distillation column. Not only can the manipulated variables reach to new steady state values, but the controlled variables can also return back to their nominal steady state values after a settling time of about 10 to 12 h. The  $CS_{D/QR}$  structure can make the composition of the controlled components to turn back to their nominal steady state values but leads to serious oscillatory responses and settling times up to 30 h. The  $CS_{D/B}$  structure leads to divergent responses and fails to maintain the composition of the controlled components. To keep the article concise, the other dynamic responses for feed composition disturbances are given in Figures S2–S19 of Supporting Information.

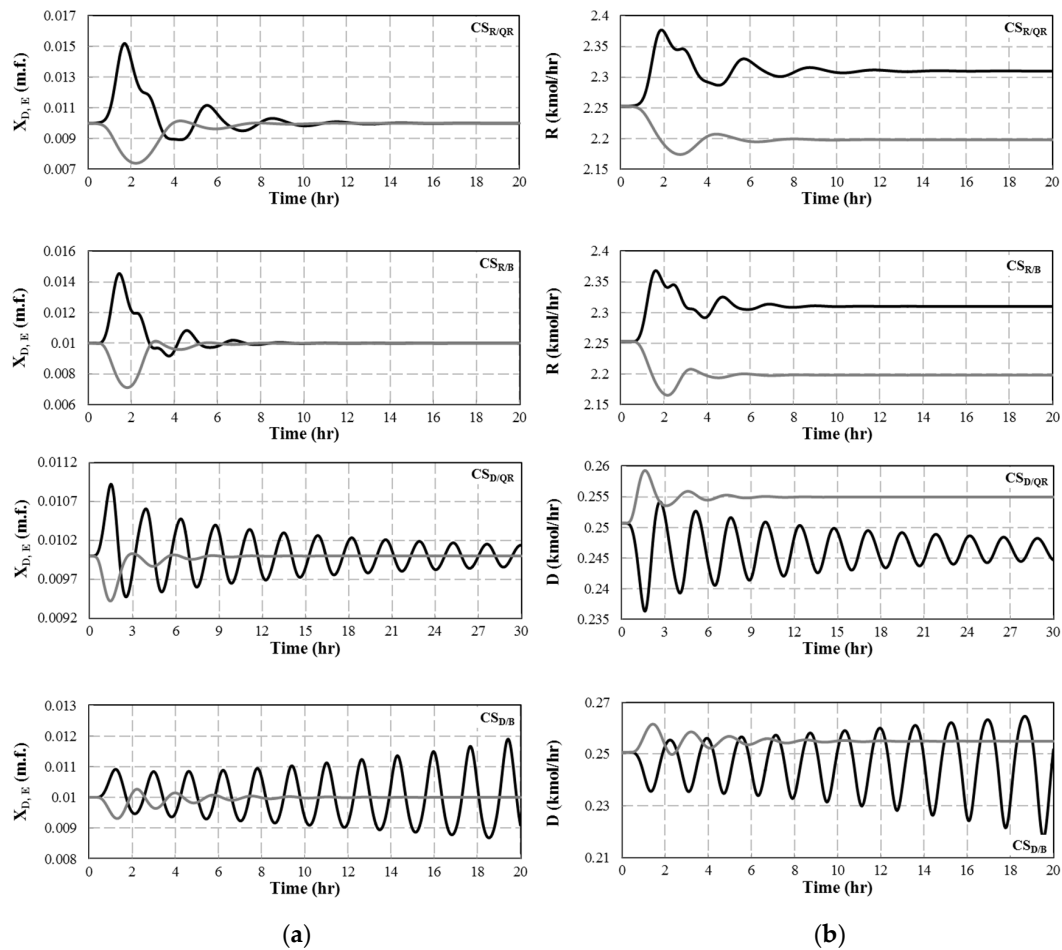


**Figure 7.** Dynamic responses of the top control loop of the MEPB Kaibel distillation column controlled, respectively, under the  $CS_{R/QR}$ ,  $CS_{R/B}$ ,  $CS_{D/QR}$ , and  $CS_{D/B}$  structures after facing a  $\pm 5\%$  variation in E feed composition (+5%: black curves and -5%: grey curves): (a) controlled variables; (b) manipulated variables.

In Table 3, the integrated absolute error (IAE) of the controlled components for a  $\pm 5\%$  variation in the composition of components M, E, P, and B are tabulated. Except the  $CS_{D/B}$  structure, the  $CS_{D/QR}$  structure retains the largest IAE among the remaining three control structures because of its serious oscillatory responses. Besides, the  $CS_{R/B}$  structure displays slightly smaller IAE than the  $CS_{R/QR}$  structure.

**Table 3.** Integrated absolute error (IAE) of the Controlled Components for a  $\pm 5\%$  Variation in the Composition of Components M, E, P, and B.

Scenario	Product	IAE			
		$CS_{R/QR}$	$CS_{R/B}$	$CS_{D/QR}$	$CS_{D/B}$
+5% $Z_M$	$X_{D,E}$	0.2108	0.1553	0.2865	0.3051
	$X_{S1,E}$	0.1185	0.0881	0.1495	0.2192
	$X_{S2,P}$	0.0563	0.0415	0.2198	0.2835
	$X_{B,P}$	0.1258	0.0729	0.5452	0.1624
	$X_{Ptop,P}$	0.0031	0.0032	0.0094	0.0181
-5% $Z_M$	$X_{D,E}$	0.2041	0.163	0.2407	0.2563
	$X_{S1,E}$	0.1082	0.0892	0.0775	0.1657
	$X_{S2,P}$	0.0337	0.0254	0.0635	0.1254
	$X_{B,P}$	0.0821	0.0745	0.1424	0.0968
	$X_{Ptop,P}$	0.0024	0.0026	0.0041	0.0097

Table 3. Cont.

Scenario	Product	IAE			
		CS <sub>R/QR</sub>	CS <sub>R/B</sub>	CS <sub>D/QR</sub>	CS <sub>D/B</sub>
+5% Z <sub>E</sub>	X <sub>D, E</sub>	0.992	0.6495	0.4877	-
	X <sub>S1, E</sub>	0.6	0.4594	0.6726	-
	X <sub>S2, P</sub>	0.3348	0.188	1.0907	-
	X <sub>B, P</sub>	0.9535	0.1127	2.6314	-
	X <sub>Ptop, P</sub>	0.011	0.0099	0.037	-
−5% Z <sub>E</sub>	X <sub>D, E</sub>	0.5736	0.4535	0.0919	0.1304
	X <sub>S1, E</sub>	0.2721	0.246	0.1433	0.1698
	X <sub>S2, P</sub>	0.1255	0.0978	0.1248	0.1117
	X <sub>B, P</sub>	0.4682	0.08	0.4724	0.0863
	X <sub>Ptop, P</sub>	0.004	0.0056	0.0039	0.0079
+5% Z <sub>P</sub>	X <sub>D, E</sub>	0.1495	0.1158	0.0816	0.0825
	X <sub>S1, E</sub>	0.1041	0.0978	0.0616	0.079
	X <sub>S2, P</sub>	0.0811	0.0618	0.093	0.0744
	X <sub>B, P</sub>	0.1433	0.0771	0.1809	0.0593
	X <sub>Ptop, P</sub>	0.003	0.0033	0.004	0.0052
−5% Z <sub>P</sub>	X <sub>D, E</sub>	0.2177	0.1277	0.2522	0.314
	X <sub>S1, E</sub>	0.1679	0.1133	0.3038	0.3547
	X <sub>S2, P</sub>	0.111	0.061	0.5545	0.5104
	X <sub>B, P</sub>	0.2271	0.0784	1.2866	0.2735
	X <sub>Ptop, P</sub>	0.004	0.0033	0.0199	0.0284
+5% Z <sub>B</sub>	X <sub>D, E</sub>	0.3497	0.2689	0.0879	0.1538
	X <sub>S1, E</sub>	0.1723	0.1638	0.0845	0.1774
	X <sub>S2, P</sub>	0.1038	0.0824	0.1285	0.1735
	X <sub>B, P</sub>	0.3362	0.2296	0.4131	0.1944
	X <sub>Ptop, P</sub>	0.0037	0.0043	0.005	0.0116
−5% Z <sub>B</sub>	X <sub>D, E</sub>	0.4519	0.346	0.1823	0.4912
	X <sub>S1, E</sub>	0.2735	0.2638	0.2266	0.5687
	X <sub>S2, P</sub>	0.1683	0.1278	0.4107	0.756
	X <sub>B, P</sub>	0.4628	0.2133	1.0232	0.422
	X <sub>Ptop, P</sub>	0.0058	0.0067	0.0144	0.043
Sum		8.8164	5.4642	12.9086	-

Figure 8 displays the dynamic responses of the top control loop of the MEPB Kaibel distillation column controlled, respectively, under the CS<sub>R/QR</sub>, CS<sub>R/B</sub>, CS<sub>D/QR</sub>, and CS<sub>D/B</sub> structures in the face of a  $\pm 5\%$  variation in feed flow rate (The dynamic responses of the other control loops are given in Figures S20–S23 of Supporting Information). It can be seen that all these four control structures can maintain the composition of the controlled components, but the dynamic characteristics of the CS<sub>D/QR</sub> and CS<sub>D/B</sub> structures is slightly inferior to the CS<sub>R/QR</sub> and CS<sub>R/B</sub> structures. Table 4 lists the IAE of the controlled components for a  $\pm 5\%$  variation in the feed flow rate.

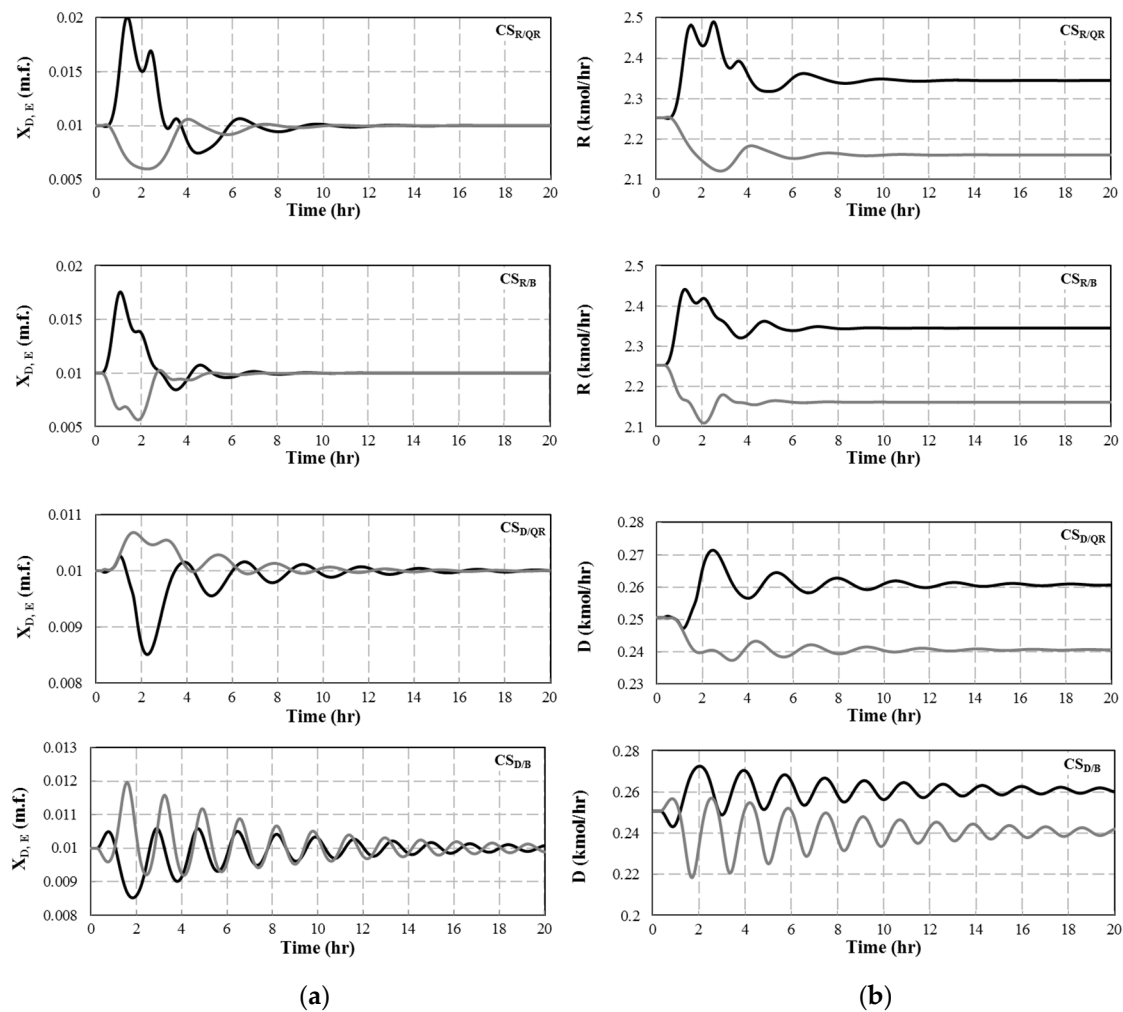


**Figure 8.** Dynamic responses of the top control loop of the MEPB Kaibel distillation column controlled, respectively, under the  $CS_{R/QR}$ ,  $CS_{R/B}$ ,  $CS_{D/QR}$ , and  $CS_{D/B}$  structures after facing a  $\pm 5\%$  variation in feed flow rate (+5%: black curves and -5%: grey curves): (a) controlled variables; (b) manipulated variables.

**Table 4.** IAE of the Controlled Components for a  $\pm 5\%$  Variation in Feed Flow Rate.

Scenario	Product	IAE			
		$CS_{R/QR}$	$CS_{R/B}$	$CS_{D/QR}$	$CS_{D/B}$
+5% $Z_F$	$X_{D,E}$	1.8270	1.1020	0.3078	0.5605
	$X_{S1,E}$	0.8488	0.6523	0.3898	0.6444
	$X_{S2,P}$	0.5816	0.2258	0.7205	0.6731
	$X_{B,P}$	1.8708	0.2409	2.2341	0.4253
	$X_{Ptop,P}$	0.0199	0.0149	0.0280	0.0418
-5% $Z_F$	$X_{D,E}$	1.0321	0.7573	0.2152	0.7070
	$X_{S1,E}$	0.4427	0.3763	0.2111	0.7684
	$X_{S2,P}$	0.2220	0.1651	0.2841	0.7336
	$X_{B,P}$	0.9831	0.1953	1.1597	0.4613
	$X_{Ptop,P}$	0.0085	0.0101	0.0111	0.0498
Sum		7.8364	3.7399	5.5615	5.0651

#### 4. Discussion

From the dynamic simulation results above, it can be observed that the  $CS_{R/QR}$  and  $CS_{R/B}$  structures are essentially superior to the  $CS_{D/QR}$  and  $CS_{D/B}$  structures. As for the main reason of causing such a great performance gap, it should be attributed to the selection of the manipulated variables of their top

control loops, that is,  $R$  is employed as manipulated variable in the former two control structures but  $D$  is selected in the latter two control structures. In fact, the reflux ratio of the MEPB Kaibel distillation column studied in the current work is as high as 8.99, which means that  $R$  is much larger than  $D$  and also implies that the open-loop gains of the top control loops of the  $CS_{R/QR}$  and  $CS_{R/B}$  structures are much higher than those of the  $CS_{D/QR}$  and  $CS_{D/B}$  structures. Therefore, when disturbances are imposed to the MEPB Kaibel distillation, the  $CS_{R/QR}$  and  $CS_{R/B}$  structures can quickly suppress the adverse effects of the disturbances on the top product and then reduce the possible adverse effects caused by the failed control of the top product to the control of the upper sidestream, lower sidestream, and bottom products. Figure 9 shows the steady state relationship between the  $R/D$  and the composition of component  $M$  of the top product when the purity of upper sidestream, lower sidestream, bottom, and prefractionator products have been maintained at their nominal steady state values. The obtained result supports well our above analyses. All in all, if one of  $R$  and  $D$  is much larger than the other, the larger one should be selected as the manipulated variable of the composition control loop to guarantee the performance of the derived composition control structure for the control of the Kaibel distillation column.

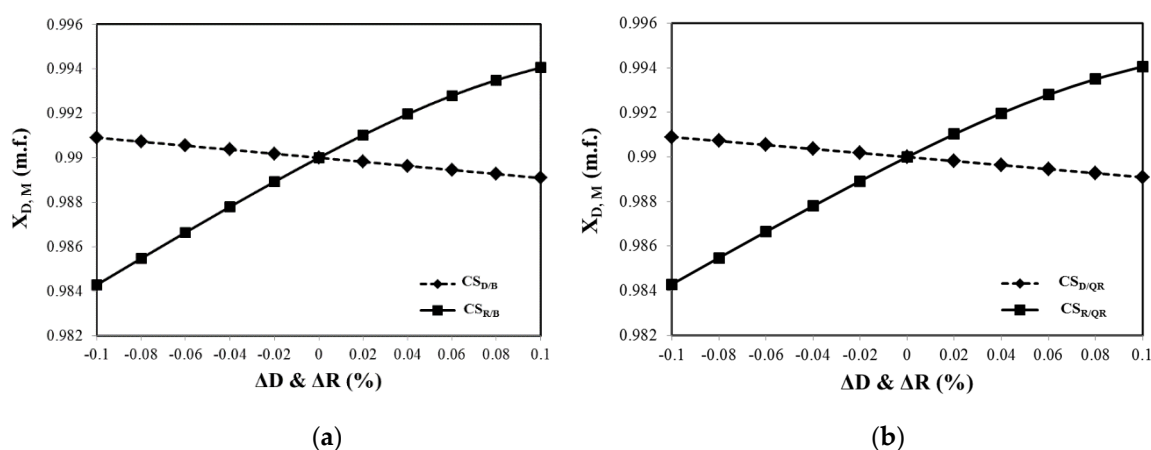


**Figure 9.** Static operation analysis of the Kaibel distillation column: (a)  $CS_{D/B}$  and  $CS_{R/B}$  structures; (b)  $CS_{D/QR}$  and  $CS_{R/QR}$  structures.

In addition, the  $CS_{R/QR}$  structure leads to slightly bigger IAE of the controlled components than the  $CS_{R/B}$  structure for the same magnitude of disturbances, which is mainly because that  $Q_R$  and  $B$  is, respectively, employed as the manipulated variable of the bottom control loop in the  $CS_{R/QR}$  and  $CS_{R/B}$  structures. More specifically, since heat transfer process is slower than valve regulation process, the control loop with  $Q_R$  as manipulated variable will unavoidably show a slower dynamic response than the control loop with  $B$  as manipulated variable. However, the difference between selecting  $Q_R$  and  $B$  as manipulated variable is not always very obvious from the difference in IAE between the  $CS_{R/QR}$  and  $CS_{R/B}$  structures obtained in the current article. Although only the MEPB Kaibel distillation column is studied in the current work, the guides obtained for developing composition control systems should be effective for different Kaibel distillation columns.

## 5. Conclusions

In the current work, the  $CS_{R/QR}$ ,  $CS_{R/B}$ ,  $CS_{D/QR}$ , and  $CS_{D/B}$  structures are proposed and systematically compared in terms of the control of a MEPB Kaibel distillation column. The similarity of these four composition control structures lies in that they include uniformly five composition control loops, i.e., the top, upper sidestream, lower sidestream, bottom, and prefractionator composition control loops. The former four control loops are, respectively, used to maintain the purity of the top, upper sidestream, lower sidestream, and bottom products, and the latter control loop is used to minimize the operation cost of the controlled Kaibel distillation column by tightly maintaining the composition of

the heavy component (Component P) at the first stage of the prefractionator. The difference of these four composition control structures lies in that different manipulated variables are employed in their top and bottom control loops (as can be seen from the subscripts to their names). According to the closed-loop simulation results, the  $CS_{R/QR}$  and  $CS_{R/B}$  structures can force the purity of the controlled components return back to their nominal steady state values with a small overshoot and relatively short settling time, however, the  $CS_{D/QR}$  and  $CS_{D/B}$  structures show serious oscillatory responses and the  $CS_{D/B}$  structure even displays divergent responses in the face of individual disturbances.

**Supplementary Materials:** The following are available online at <http://www.mdpi.com/2227-9717/8/2/218/s1>, Figure S1: A simple sequential search algorithm for the synthesis and design of the Kaibel distillation column, Figures S2–S23: Dynamic responses of the upper sidestream control loop of the MEPB Kaibel distillation column controlled, respectively, under the  $CS_{R/QR}$ ,  $CS_{R/B}$ ,  $CS_{D/QR}$ , and  $CS_{D/B}$  structures after facing step changes in feed compositions and feed flow rate. Table S1: Column dimensions of the MEPB Kaibel distillation column.

**Author Contributions:** Conceptualization, Y.Y.; Funding acquisition, Y.Y., H.C. and X.Q.; Investigation, Y.Y.; Project administration, K.H., H.C., and X.Q.; Visualization, L.Z. (Liang Zhang); Writing—original draft, Y.Y.; Writing—review and editing, L.Z. (Lijiang Zang) and S.W. All authors have read and agreed to the published version of the manuscript.

**Funding:** The research funding is from China Postdoctoral Science Foundation (No. 2019M650453), Fundamental Research Funds for the Central Universities (ZY1930), National Science Foundation of China (21808007, 21878011, 21676011, and 21576014), and Open Foundation of State Key Laboratory of Chemical Engineering (No. SKL-ChE-18B01).

**Conflicts of Interest:** The authors declare no conflict of interest.

## References

1. Kiss, A.A.; Bildea, C.S. A control perspective on process intensification in dividing-wall columns. *Chem. Eng. Process.* **2011**, *50*, 281–292. [CrossRef]
2. Yildirim, Ö.; Kiss, A.A.; Kenig, E.Y. Dividing wall columns in chemical process industry: A review on current activities. *Sep. Purif. Technol.* **2011**, *80*, 403–417. [CrossRef]
3. Dejanović, I.; Matijašević, L.; Olujić, Ž. Dividing wall column—A breakthrough towards sustainable distilling. *Chem. Eng. Process.* **2010**, *49*, 559–580. [CrossRef]
4. Olujić, Ž.; Jödecke, M.; Shilkin, A.; Schuch, G.; Kaibel, B. Equipment improvement trends in distillation. *Chem. Eng. Process.* **2009**, *48*, 1089–1104. [CrossRef]
5. Donahue, M.M.; Roach, B.J.; Downs, J.J.; Blevins, T.; Baldea, M.; Eldridge, R.B. Dividing wall column control: Common practices and key findings. *Chem. Eng. Process.* **2016**, *107*, 106–115. [CrossRef]
6. Asprion, N.; Kaibel, G. Dividing wall columns: Fundamentals and recent advances. *Chem. Eng. Process.* **2010**, *49*, 139–146. [CrossRef]
7. Dejanović, I.; Matijašević, L.J.; Halvorsen, I.J.; Skogestad, S.; Jansen, H.; Kaibel, B.; Olujić, Ž. Designing four-product dividing wall columns for separation of a multicomponent aromatics mixture. *Chem. Eng. Res. Des.* **2011**, *89*, 1155–1167. [CrossRef]
8. Tututi-Avila, S.; Domínguez-Díaz, L.A.; Medina-Herrera, N.; Jiménez-Gutiérrez, A.; Hahn, J. Dividing-wall columns: Design and control of a kaibel and a satellite distillation column for BTX separation. *Chem. Eng. Process.* **2017**, *114*, 1–15. [CrossRef]
9. Abid, F.; Shamsuzzoha, M.; Binous, H.; Alshammari, A. Optimal operation and control of four-product dividing-wall (Kaibel) distillation column. *Arabian J. Chem. Sci. Eng.* **2018**, *43*, 6067–6085. [CrossRef]
10. Qian, X.; Huang, K.; Chen, H.; Yuan, Y.; Zhang, L.; Wang, S. Intensifying Kaibel dividing-wall column via vapor recompression heat pump. *Chem. Eng. Res. Des.* **2019**, *142*, 195–203. [CrossRef]
11. Ling, H.; Qiu, J.; Hua, T.; Wang, Z. Remixing analysis of four-product dividing-wall columns. *Chem. Eng. Technol.* **2018**, *41*, 1359–1367. [CrossRef]
12. Wang, S.J.; Wong, D.S.H. Controllability and energy efficiency of a high-purity divided wall column. *Chem. Eng. Sci.* **2007**, *62*, 1010–1025. [CrossRef]
13. Ling, H.; Luyben, W.L. Temperature control of the BTX divided-wall column. *Ind. Eng. Chem. Res.* **2010**, *49*, 189–203. [CrossRef]

14. Luan, S.; Huang, K.; Wu, N. Operation of dividing-wall columns. 1. A simplified temperature difference control scheme. *Ind. Eng. Chem. Res.* **2013**, *52*, 2642–2660. [\[CrossRef\]](#)
15. Wu, N.; Huang, K.; Luan, S. Operation of dividing-wall distillation columns. 2. A double temperature difference control scheme. *Ind. Eng. Chem. Res.* **2013**, *52*, 5365–5383. [\[CrossRef\]](#)
16. Yuan, Y.; Huang, K. Operation of dividing-wall distillation columns. 3. A simplified double temperature difference control scheme. *Ind. Eng. Chem. Res.* **2014**, *53*, 15969–15979. [\[CrossRef\]](#)
17. Dwivedi, D.; Strandberg, J.P.; Halvorsen, I.J.; Skogestad, S. Steady state and dynamic operation of four-product dividing-wall (Kaibel) columns: Experimental verification. *Ind. Eng. Chem. Res.* **2012**, *51*, 15696–15709. [\[CrossRef\]](#)
18. Qian, X.; Jia, S.; Skogestad, S.; Yuan, X. Control structure selection for four-product Kaibel column. *Comput. Chem. Eng.* **2016**, *93*, 372–381. [\[CrossRef\]](#)
19. Fan, G.; Jiang, W.; Qian, X. Comparison of stabilizing control structures for four-product Kaibel column. *Chem. Eng. Res. Des.* **2016**, *109*, 675–685. [\[CrossRef\]](#)
20. Pan, H.; Wu, X.; Qiu, J.; He, G.; Ling, H. Pressure compensated temperature control of Kaibel divided-wall column. *Chem. Eng. Sci.* **2019**, *203*, 321–332. [\[CrossRef\]](#)
21. Qian, X.; Huang, K.; Jia, S.; Chen, H.; Yuan, Y.; Zhang, L.; Wang, S. Composition/temperature cascade control for a Kaibel dividing-wall distillation column by combining PI controllers and model predictive control integrated with soft sensor. *Comput. Chem. Eng.* **2019**, *126*, 292–303. [\[CrossRef\]](#)
22. Skogestad, S. Control structure design for complete chemical plants. *Comput. Chem. Eng.* **2004**, *28*, 219–234. [\[CrossRef\]](#)
23. Ling, H.; Luyben, W.L. New control structure for divided-wall columns. *Ind. Eng. Chem. Res.* **2009**, *48*, 6034–6049. [\[CrossRef\]](#)
24. Wang, P.; Chen, H.; Wang, Y.; Zhang, L.; Huang, K.; Wang, S.J. A simple algorithm for the design of fully thermally coupled distillation columns (FTCDC). *Chem. Eng. Commun.* **2012**, *199*, 608–627. [\[CrossRef\]](#)
25. Luyben, W.L. *Distillation Design and Control using Aspen Simulation*; John Wiley & Sons: New York, NY, USA, 2006.



© 2020 by the authors. Licensee MDPI, Basel, Switzerland. This article is an open access article distributed under the terms and conditions of the Creative Commons Attribution (CC BY) license (<http://creativecommons.org/licenses/by/4.0/>).